



Assessment of brain tumors by magnetic resonance dynamic susceptibility contrast perfusion-weighted imaging and computed tomography perfusion: a comparison study

Elisa Scola¹ · Ilaria Desideri¹ · Andrea Bianchi¹ · Davide Gadda¹ · Giorgio Busto¹ · Alessandro Fiorenza² · Tommaso Amadori² · Sara Mancini² · Vittorio Miele³ · Enrico Fainardi^{1,4}

Received: 21 September 2021 / Accepted: 11 February 2022 / Published online: 20 April 2022
© Italian Society of Medical Radiology 2022

Abstract

Purpose To investigate the association and agreement between magnetic resonance dynamic susceptibility contrast perfusion-weighted imaging (DSC-PWI) and computed tomography perfusion (CTP) in determining vascularity and permeability of primary and secondary brain tumors.

Material and methods DSC-PWI and CTP studies from 97 patients with high-grade glioma, low-grade glioma and solitary brain metastasis were retrospectively reviewed. Normalized cerebral blood flow (nCBF), cerebral blood volume (nCBV), capillary transfer constant (nK2) and permeability surface area product (nPS) values were obtained. Variables among groups were compared, and correlation and agreement between DSC-PWI and CTP were tested.

Results All DSC-PWI and CTP parameters were higher in high-grade than in low-grade gliomas ($p < 0.01$ and $p < 0.001$). Metastases had greater DSC-PWI nCBV ($p < 0.05$), nCTP-CBF ($p < 0.05$), nCTP-CBV ($p < 0.01$) and nCTP-PS ($p < 0.0001$) than low-grade gliomas and more elevated nCTP-PS ($p < 0.01$) than high-grade gliomas. The correlation was strong between DSC-PWI nCBF and CTP nCBF ($r = 0.79$; $p < 0.00001$) and between DSC-PWI nCBV and CTP nCBV ($r = 0.83$; $p < 0.00001$), weaker between DSC-PWI nK2 and CTP nPS ($r = 0.29$; $p < 0.01$). Bland–Altman plots indicated that the agreement was strong between DSC-PWI nCBF and CTP nCBF, good between DSC-PWI nCBV and CTP nCBV and poorer between DSC-PWI nK2 and CTP nPS.

Conclusion DSC-PWI and CTP CBF and CBV maps were comparable and interchangeable in the assessment of tumor vascularity, unlike DSC-PWI K2 and CTP PS maps that were more discordant in the analysis of tumor permeability. CTP could be an alternative method to quantify tumor neoangiogenesis when MRI is not available or when the patient does not tolerate it.

Keywords Computed tomography perfusion · Magnetic resonance perfusion-weighted Imaging · Brain tumors · Agreement

Introduction

Perfusion imaging allows the identification of biological properties of brain tumors that are otherwise non depictable on conventional imaging. Concerning magnetic resonance imaging (MRI), vascularity of brain tumors is explored with perfusion-weighted imaging (PWI) by using two different methods, dynamic susceptibility contrast (DSC) and dynamic contrast enhanced (DCE), which are both based on gadolinium injection [1, 2]. However, DSC has been the most extensively PWI technique applied in the assessment of brain tumors due to its ability in quantifying the tumor vascular supply [3]. DSC-PWI may identify glioma grade and survival, distinguish gliomas from other brain lesions, predict the tumor response to antiangiogenic therapy and

✉ Elisa Scola
scolae@aou-careggi.toscana.it

¹ Struttura Organizzativa Dipartimentale di Neuroradiologia, Dipartimento di Radiologia, Ospedale Universitario Careggi, Largo Brambilla 3, 50134 Florence, Italy

² Radiodiagnostic Unit N. 2, Department of Experimental and Clinical Biomedical Sciences, University of Florence, Florence, Italy

³ Department of Emergency Radiology, Careggi University Hospital, Florence, Italy

⁴ Neuroradiology Unit, Department of Experimental and Clinical Biomedical Sciences “Mario Serio”, University of Florence, Florence, Italy

differentiate post-treatment changes from tumor progression and recurrence [1, 4]. Therefore, DSC-PWI has been demonstrated to increase the reliance of neuroradiologists and physicians in the management of brain tumors in 40% and 56% of cases, modifying the treatment in 8.5% of patients [5]. In addition, although with lower accuracy than DCE-PWI [6], DSC-PWI is able to evaluate vessel permeability calculating capillary transfer constant (K_2) parameter by a leakage-correction algorithm [7]. On the other hand, brain tumor hemodynamics can also be measured with perfusion-computed tomography (CTP) that has been reported to be a useful tool for differential diagnosis and prediction of tumor grading, prognosis, and treatment response [8–12]. Furthermore, CTP can study vascular permeability, preferably with a two-phase acquisition protocol that allows to obtain permeability surface area product (PS) parameter [2, 10]. Another advantage of CTP is the linear relationship between the iodine contrast concentration and CT attenuation that provides a direct measurement of perfusion parameters [2]. For these reasons, CTP has been proposed as an alternative technique for the assessment of brain tumor vascularity and permeability in patients with contraindication to MRI [10].

Nevertheless, a few data are currently available on the agreement between CTP and PWI parameters that are difficult to compare since, despite both PWI and CTP tracking the contrast delivery to tissues during and after the arrival of the contrast bolus, these two techniques have several differences in acquisition and computation models [1, 2]. In fact, only three studies have previously been published testing the correspondence between PWI and CTP parameters in brain tumors. Of these, only one described the correlation between DSC-PWI and CTP cerebral blood volume (CBV) in patients with high-grade glioma [13], whereas the others estimated the relationships between DCE-PWI and CTP permeability values in patients with brain metastasis and glioblastoma [14, 15]. Based on these observations, the present study aims to assess the correlation and agreement of pharmacokinetic parameters derived from DSC-PWI and CTP in patients with both primary and secondary brain tumors.

Material and methods

Patients

Ninety-seven patients (56 males and 41 females; mean age \pm SD = 61.1 \pm 13.2 years) with suspected solitary intra-axial brain tumor at admission CT and/or MRI were included in the study and underwent brain DSC-PWI and CTP. DSC-PWI and CTP studies from all patients were retrospectively reviewed. CTP was acquired within 5 days after DSC-PWI, always prior to surgery and to any steroid or chemotherapy or radiation treatment. All patients underwent surgical

biopsy or tumor removal within 7 days after CTP examination. Histologic analyses were based on the World Health Organization (WHO) classification and were obtained after total surgical resection of the tumor in 36 patients, partial surgical resection in 39 patients and stereotaxic biopsy in 22 patients. Fifty-eight patients were diagnosed with WHO grade IV glioma (glioblastoma IDH-wildtype), 15 patients with grade III glioma (5 anaplastic astrocytoma IDH-mutant, 2 anaplastic ependymoma, 8 anaplastic oligodendroglioma IDH-mutant and 1p/19q-codeleted), 12 patients with low-grade glioma (4 diffuse astrocytoma IDH-mutant, 1 oligoastrocytoma, 7 oligodendroglioma IDH-mutant and 1p/19q-codeleted) and 12 patients with metastatic brain lesions (9 with primitive pulmonary tumor, 1 renal tumor, 1 breast cancer and 1 colon cancer). Patients were then grouped according to histological diagnosis in high-grade gliomas (WHO IV and III grade), low-grade gliomas (WHO II and I) and isolated metastases (all patients with secondary brain lesion). Karnofsky performance status at entry ranged from 50 to 100%. Our institutional review board approved this prospective study.

Imaging protocol

MRI were acquired with a 1.5 T Achieva scanner (Philips Medical Systems, Best, the Netherlands). MRI protocol included the following sequences: axial T1-weighted spin-echo (SE), axial T2-weighted SE, coronal FLAIR, and diffusion-weighted imaging (DWI). PWI was performed with DSC technique with echo planar imaging (EPI) Fast Field (Gradient)-Echo sequence of 25 adjacent slices with thickness of 5 mm and 0 gap, 40 dynamics, 90 \times 128 matrix, time to repetition (TR) 1877 ms, time to echo (TE) 40 ms, NSA 1, flip angle 75°, turbo factor 47 and EPI factor 47. The sequence was obtained during intravenous administration of a 0.1-mmol/kg bolus of Gadoteridol (Prohance, Bracco) at a 4.0 ml/s rate, with 16 s delay followed by 20 ml saline at the same rate, using a power injector. Total acquisition time was 1 min and 24 s. Postcontrast axial T1-weighted images were acquired after the acquisition of DSC-PWI sequence. All CTP studies were performed using a multidetector-row CT scanner (CT HiSpeed ZX/i; GE Healthcare, Milwaukee, Wisconsin) equipped for CT perfusion imaging (CT Perfusion; GE Medical System, Milwaukee, Wis). CTP consisted in a two-phase protocol (80 kV, 140 mA, 0.5 rotation time, 5 mm slice thickness with 8 cm head coverage) located at the tumor level and including the largest volume of neoplastic tissue. The two-phase acquisition consisted of a first phase every 2.8 s for 60 s and an additional second phase every 15 s for 90 s. The acquisition started 5 s after the automatic injection of a bolus of 40 mL of nonionic contrast agent (Iomeron 300 mg/mL, Bracco Imaging SpA) followed by a saline flush of 40 mL at the rate of 4 mL/s. The total scan

duration was 150 s. All CTP source images were reconstructed with the standard filter and DFOV of 25 cm.

Image post-processing and analysis

DSC-PWI was analyzed with a dedicated software package (Olea SPHERE®, Olea Medical®, La Ciotat, France). Parametric maps of cerebral blood flow (CBF) and CBV were then obtained using the standard truncated singular value decomposition algorithm (sSVD) for deconvolution [16] and an automatic method to obtain the arterial input function (AIF). The same method was applied to calculate the permeability K_2 maps [7]. K_2 is the capillary transfer constant describing the movement of contrast from extravascular space back into vessels. In order to avoid the underestimation of CBV due to contrast leakage through the damaged blood brain barrier in tumors, a mathematical correction of leakage was applied to CBV maps. Therefore, the corrected CBV map derived from K_2 permeability maps were obtained. Perfusion parametric maps were co-registered to postcontrast axial T1-weighted images. CT perfusion maps of CBF, CBV and PS were computed using a commercially available delay-insensitive deconvolution software (CT Perfusion 4D, GE Healthcare, Milwaukee, Wisconsin). Arterial and venous time-attenuation curves were measured positioning 2×2 voxels (in-slice) Regions of Interest (ROIs), respectively, on the basilar artery, internal carotid artery, on anterior cerebral artery and on the posterior superior sagittal sinus. CTP CBF, CBV and PS maps were calculated by deconvolving the arterial time-attenuation curve with the tissue time-attenuation curve with a two-compartmental model. Average CTP maps were created by averaging the cine (dynamic) CTP source images over the duration of the first pass of contrast. Large blood vessels were automatically excluded from calculation by the software [17, 18]. As shown in Fig. 1, two different regions of interest (ROI) larger than 1 cm^2 were manually drawn on contrast-enhanced T1-weighted images and on average CTP images that were co-registered with DSC-PWI and CTP parametric maps, respectively. Average CTP images were chosen due to their optimal contrast resolution of tumor borders. The first ROI was drawn on every section in which the enhancing or non-enhancing tumor solid tissue was visible, avoiding necrotic and cystic areas, and carefully selecting the matching CT and MR slices. The second ROI, mirroring the tumor region, was delineated on the apparently normal brain tissue on the contralateral hemisphere. Regional CBF, CBV and K_2 and PS absolute levels were measured in both tumor and apparently normal tissue. Normalized values both for DSC-PWI (PWI nCBF; PWI nCBV; and PWI n K_2) and CTP (CTP nCBF; CTP nCBV; and CTP nPS) were then obtained by

dividing tumor and contralateral absolute levels. CBF, CBV, K_2 and PS values were expressed in mL/100 g/min, mL/100 g, s and mL/100 g/min, respectively.

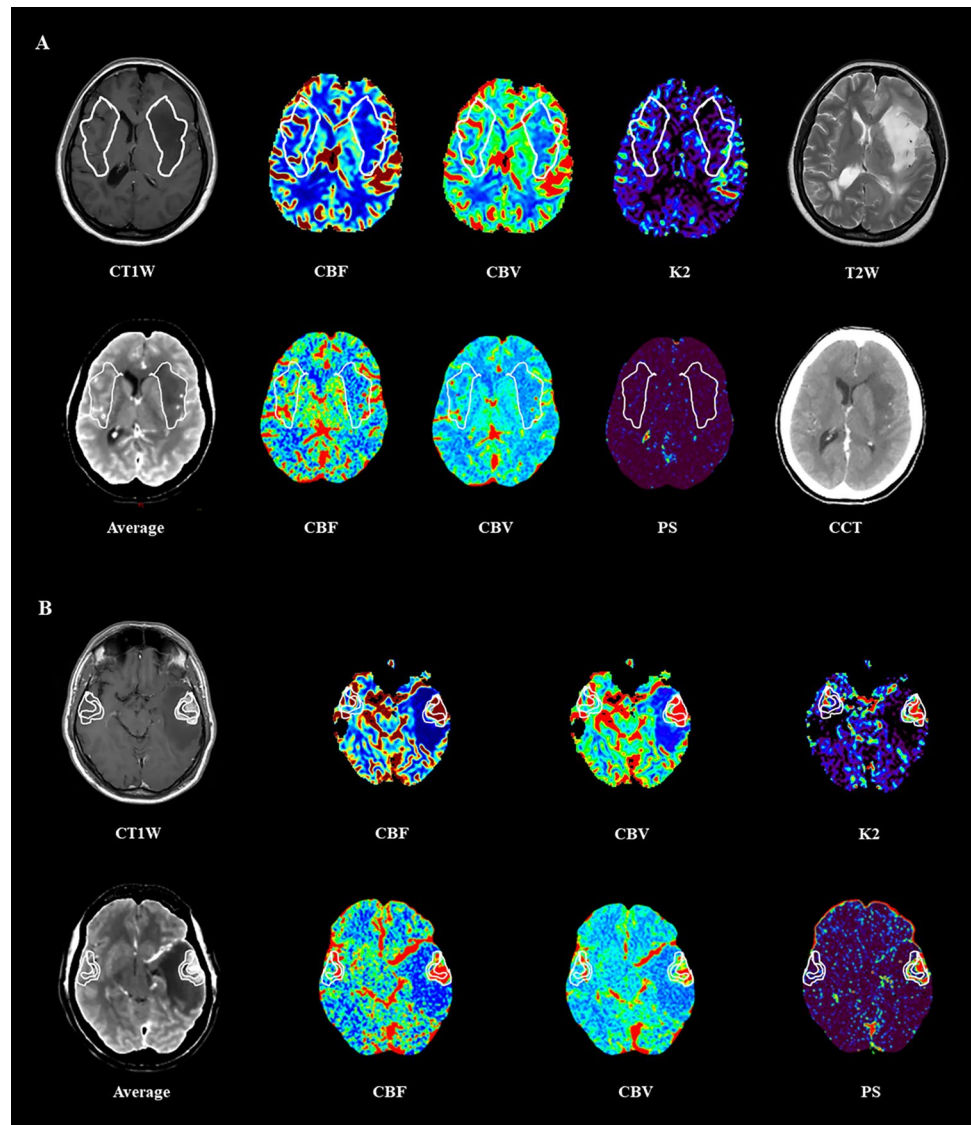
Statistical analysis

Data were checked for normality using the Kolmogorov–Smirnov test. As normality of data distribution was rejected in several variables, statistical analysis was performed by a nonparametric statistical approach. Continuous variables were compared using the Kruskal–Wallis test followed the Mann–Whitney U test with Bonferroni correction for multiple comparisons. Correlation between the continuous variables was assessed by the Spearman's correlation test. The agreement between DSC-PWI and CTP variables was evaluated by the Bland–Altman test. A value of $p < 0.05$ was accepted as statistically significant. Statistical analysis was performed with GraphPad Prism.

Results

A total of 97 subjects were included in the study of whom 73 had high-grade gliomas, 12 had low-grade gliomas and 12 had solitary brain metastases. Cohort demographic, clinical and radiological features are listed in Table 1. As indicated in Fig. 2, a statistical difference was found for DSC-PWI nCBF ($p < 0.001$), DSC-PWI nCBV levels, DSC-PWI n K_2 , CTP nCBF, CTP nCBV ($p < 0.01$) and CTP nPS ($p < 0.001$) among high-grade gliomas, low-grade gliomas and metastases. In particular, high-grade gliomas had significantly higher values for DSC-PWI nCBF, DSC-PWI nCBV ($p < 0.001$) and DSC-PWI n K_2 ($p < 0.01$) than low-grade gliomas (Fig. 2, panel A), whereas DSC-PWI nCBV levels were statistically more elevated in metastases than in low-grade gliomas ($p < 0.05$). On the other hand, while high-grade gliomas had significantly greater CTP nCBF ($p < 0.01$), CTP nCBV ($p < 0.001$) and CTP nPS ($p < 0.01$) levels than in low-grade glioma, metastases had more increased CTP nCBF ($p < 0.05$), CTP nCBV ($p < 0.01$) and CTP nPS ($p < 0.0001$) values than low-grade gliomas and more prominent CTP nPS levels than high-grade gliomas (Fig. 2, panel B). A strong positive correlation was detected between DSC-PWI nCBF and CTP nCBF, as well as between DSC-PWI nCBV and CTP nCBV values ($p < 0.00001$), whereas less pronounced ($p < 0.01$) was the association between DSC-PWI n K_2 and CTP nPS levels (Fig. 3). As shown by bias and 95% limits of agreement values of Bland–Altman plots (Fig. 4), the agreement was strong between DSC-PWI nCBF and CTP nCBF, good between DSC-PWI nCBV and CTP nCBV and poorer between DSC-PWI n K_2 and CTP nPS levels.

Fig. 1 Tumor lesion segmentation on magnetic resonance dynamic susceptibility contrast perfusion-weighted imaging (PWI) and computed tomography perfusion (CTP) in a 43-year-old patient with low-grade glioma (Diffuse Astrocytoma IDH-mutant) located in left insular lobe (Panel A) and in a 61-year-old patient with high-grade glioma (Glioblastoma IDH-wildtype) placed in left temporal lobe (Panel B)



Discussion

The purpose of the current study was to analyze the level of correlation and agreement of perfusion parameters derived from DSC-PWI and CTP for verifying whether these two techniques are comparable and interchangeable in the assessment of tumor vascularity and permeability in primary and secondary brain malignancies. DSC-PWI and CTP showed similar results when nCBV, nCBF and permeability in high-grade and low-grade gliomas were compared given that all these parameters were higher in high-grade than in low-grade gliomas. These findings are concordant with data coming from previous studies. A recent meta-analysis found that DSC-PWI CBV had 92% sensitivity and 81% specificity in discriminating between high-grade and low-grade gliomas [19] and DSC-PWI CBF was demonstrated to enhance with increasing

glioma grade [20–22]. In addition, DSC-PWI-derived leakage coefficient K2 was reported to be significantly greater in high-grade than in low-grade gliomas [21, 23]. Finally, increased intralesional levels of CBF, CBV and PS values in high-grade than in low-grade gliomas were observed in prior CTP studies obtained with one-phase [8] or two-phase [24] acquisition protocol. Collectively, these findings confirm that an increase in CBF, CBV and permeability is related to neoangiogenesis, with increased micro-vessel density and capillary permeability, that characterizes high-grade gliomas [1, 2, 9, 10]. Conversely, DSC-PWI and CTP provided the discordant results when metastases were compared with high-grade and low-grade gliomas. In fact, while nCBF and nCBV values derived from DSC-PWI and CTP were equivalent in metastases and high-grade gliomas, and DSC-PWI and CTP nCBV levels were higher in metastases than in low-grade gliomas,

Table 1 Demographic, clinical and radiological characteristics in 97 patients with brain tumors

	High grade (<i>n</i> = 73)	Low grade (<i>n</i> = 12)	Metastases (<i>n</i> = 12)
Sex: female/male	34/39	5/7	2/10
Age, years (mean ± SD)	62.8 ± 12.8	46.5 ± 10.9	64.9 ± 7.1
WHO grade (%)			
II	/	12/12 (100%)	/
III	15/73 (20.5%)	/	/
IV	58/73 (79.5%)	/	/
Karnofsky performance status (median, IQR, mean ± SD, range)	80, 70–90, 76.3 ± 14.6, 40–100	90, 77.5–90, 85.0 ± 10.0, 70–100	80, 70–82.5, 78.0 ± 9.0, 60–90
PWI nCBF: mL/100 g/min (median, IQR, mean ± SD, range)	2.2, 1.6–2.8, 2.2 ± 0.9, 0.5–4.4	1.1, 1.0–1.5, 1.3 ± 0.3, 0.8–1.8	1.7, 1.3–2.2, 2.3 ± 2.0, 0.5–8.2
PWI nCBV: mL/100 g (median, IQR, mean ± SD, range)	2.3, 1.8–3.0, 2.4 ± 0.9, 0.6–4.8	1.2, 1.0–1.6, 1.3 ± 0.4, 0.9–2.1	1.9, 1.6–2.2, 2.3 ± 1.8, 0.6–7.4
PWI nK2: mL/100 g/min (median, IQR, mean ± SD, range)	2.8, 1.5–6.4, 4.3 ± 3.8, 0.5–14.5	1.3, 1.1–1.6, 1.4 ± 0.5, 0.7–2.2	4.2, 1.7–9.0, 5.6 ± 5.1, 0.4–17.3
CTP nCBF: mL/100 g/min (median, IQR, mean ± SD, range)	2.1, 1.8–2.6, 2.2 ± 1.0, 0.4–6.3	1.1, 1.0–1.5, 1.3 ± 0.6, 0.5–2.6	1.8, 1.4–2.4, 2.6 ± 2.7, 0.9–11.0
CTP nCBV: mL/100 g (median, IQR, mean ± SD, range)	2.2, 1.9–2.8, 2.3 ± 0.9, 0.5–6.5	1.1, 0.9–1.5, 1.3 ± 0.6, 0.6–2.8	2.4, 1.9–2.5, 3.5 ± 4.5, 1.3–17.6
CTP nPS: mL/100 g/min (median, IQR, mean ± SD, range)	6.1, 3.5–8.7, 6.4 ± 3.7, 0.9–20.1	1.1, 1.0–1.8, 1.6 ± 1.2, 0.8–4.7	10.6, 9.5–16.4, 23.2 ± 36.9, 3.9–138.1

High Grade = high-grade gliomas; Low grade = low-grade gliomas; SD = standard deviation; WHO = World Health Organization; PWI = magnetic resonance dynamic susceptibility contrast perfusion-weighted imaging; IQR = interquartile range; nCBF = normalized cerebral blood flow; nCBV = normalized cerebral blood volume; nK2 = normalized capillary transfer constant; CTP = CT perfusion; nPS = normalized permeability surface area product

nCBF values were greater in metastases than in low-grade gliomas when assessed by CTP but comparable between these two groups when assessed by PWI. More important, CTP nPS values were more elevated in metastases than in high-grade and low-grade gliomas, but DSC-PWI K2 levels were not. Conflicting findings were obtained in previous publications in which DSC-PWI and CTP parameters were used in the differential diagnosis between metastases and gliomas. No difference was observed for CBF and CBV values among metastases, high-grade and low-grade gliomas in former works performed with DSC-PWI [25] and one-phase CTP [8, 26]. Nevertheless, other studies performed with DSC-PWI [28] and one-phase CTP [27] showed more elevated CBF and CBV levels in high-grade gliomas than in metastases. In addition, some investigators did not demonstrate any difference in permeability between metastases and high-grade gliomas with DCE-PWI volume transfer constant (K^{trans}) [29] and one-phase CTP PS [8, 26, 27], whereas others reported higher DCE-PWI K^{trans} levels in high-grade gliomas than in metastases [30]. Only one study, performed with CTP K^{trans} obtained with a one-phase acquisition protocol, was consistent with our data showing greater permeability values in metastases than in high-grade gliomas [31]. A conceivable explanation for these discrepancies among various studies is the remarkable difference in models and in post-processing

methods utilized for calculating tumor vascular permeability and in patient selection among the various studies. In any case, the higher CTP nPS values we found in metastases compared to high-grade gliomas may be related to the well-known heterogeneity of tumor brain microenvironment that is different between primary tumors and metastases and likely promotes distinct level of blood–brain barrier (BBB) leakage [32, 33]. Convergent and divergent results for nCBF and nCBV and for normalized permeability, respectively, obtained with DSC-PWI and CTP in our examination of continuous variables were reflected by the analysis of correlation and agreement between DSC-PWI and CTP parameters. The demonstration of a strong positive correlation between nCBF and nCBV values derived from DSC-PWI and CTP was in agreement with a previous study [13] in which, however, CTP was acquired with a one-phase protocol and only patients with high-grade glioma were examined. On the contrary, the weaker direct association detected between DSC-PWI nK2 and CTP nPS levels did not confirm prior observations where DCE-PWI K^{trans} were compared with two-phase CTP K^{trans} values [14] and DCE-PWI K^{trans} were correlated with one-phase CTP nPS value [15]. On the other hand, the high agreement we found between nCBF and nCBV values only partially corresponded to the results of the previous study of De Simone and colleagues [13] showing lower nCBV

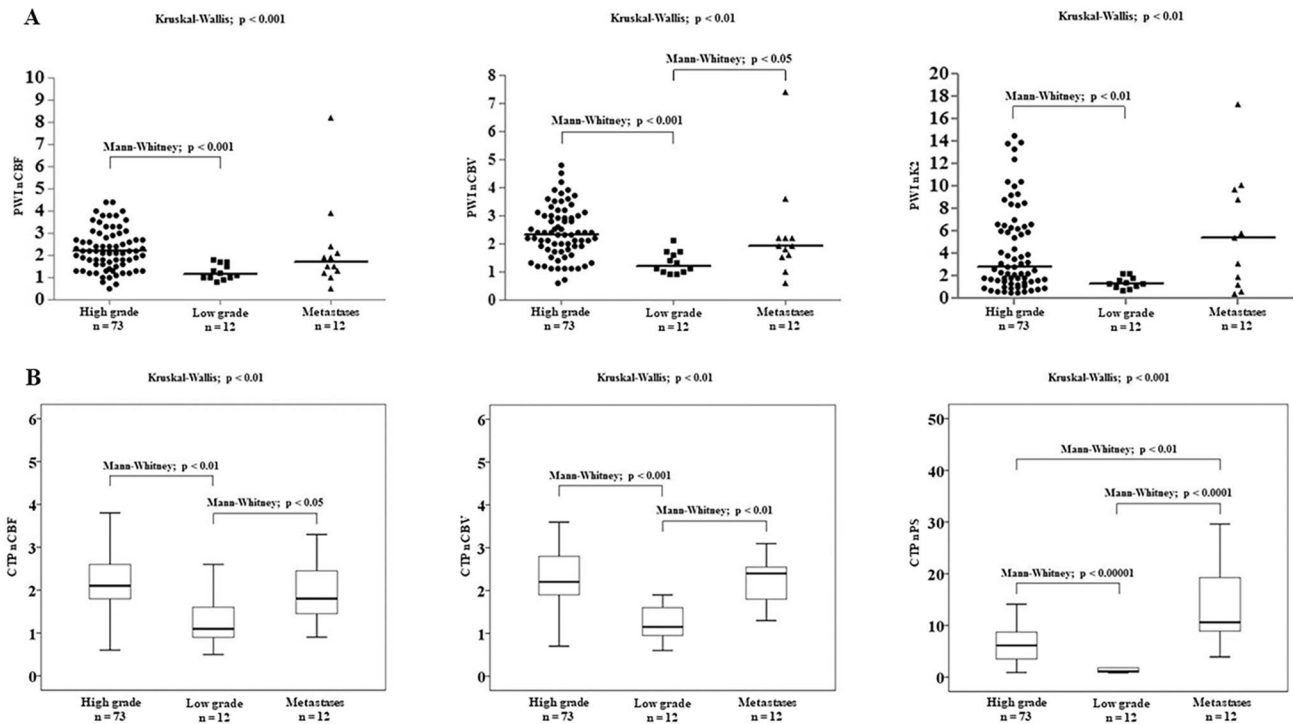


Fig. 2 Panel **A** Scatter plots showing magnetic resonance dynamic susceptibility contrast perfusion-weighted imaging (PWI) normalized cerebral blood flow (nCBF), normalized cerebral blood volume (nCBV) and normalized capillary transfer constant (nK2) values in patients with high-grade gliomas (High grade), low-grade gliomas (Low grade) and metastases. The horizontal line marks the median. Panel **B** Box plots illustrating computed tomography perfusion (CTP)

nCBF, nCBV and normalized permeability surface area product (nPS) values in patients with high-grade gliomas (High grade), low-grade gliomas (Low grade) and metastases. The boundaries of the boxes represent the 25th–75th quartile. The line within the box indicates the median. The vertical lines above and below the box correspond to the highest and lowest values, excluding outliers

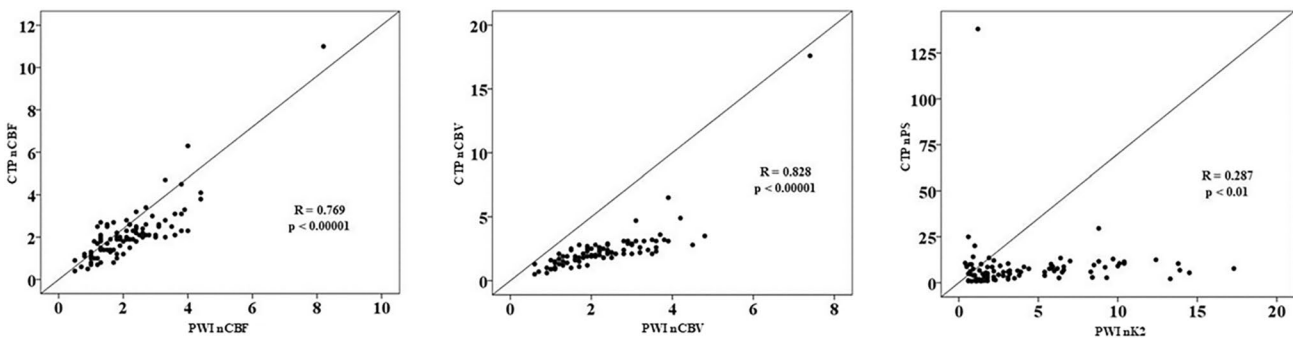


Fig. 3 Relationship between computed tomography perfusion (CTP) normalized cerebral blood flow (nCBF), normalized cerebral blood volume (nCBV) normalized permeability surface area product (nPS) values (y-axis) and magnetic resonance dynamic susceptibility con-

trast perfusion-weighted imaging (PWI) nCBF, nCBV and normalized capillary transfer constant (nK2) values (x-axis), respectively, in 97 patients with brain tumors

levels for DSC-PWI than CTP, likely due to the lack of a correction for contrast extravasation leading to an underestimation of CBV [7, 34]. In addition, the lower agreement we observed DSC-PWI nK2 and CTP nPS values was in contrast with the two already cited publications

demonstrating a good agreement DCE-PWI K^{trans} and two-phase CTP K^{trans} [14] and one-phase CTP nPS levels [15], respectively. Again, these discrepancies can be explained by methodological differences in evaluating microvascular permeability across various studies. In particular, patient

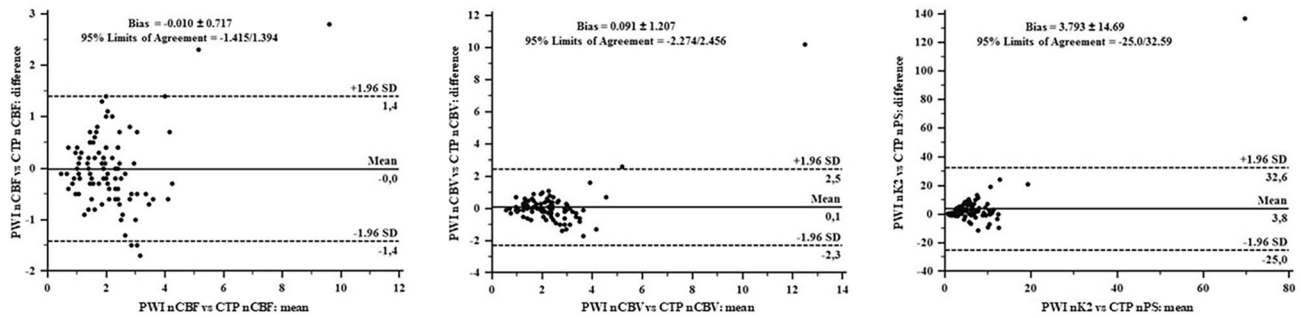


Fig. 4 Bland–Altman plots representing the level of agreement between magnetic resonance dynamic susceptibility contrast perfusion-weighted imaging (PWI) normalized cerebral blood flow (nCBF), normalized cerebral blood volume (nCBV) and normalized capillary transfer constant (nK2) values and illustrating computed tomography perfusion (CTP) nCBF, nCBV and normalized permeability surface area product (nPS) values, respectively, 97 patients with brain tumors. The mean and the difference of results obtained with the two methods (PWI and CTP) are reported on *x*-axis and *y*-axis, respectively. The solid line corresponds to bias. The dashed lines indicate the upper and the lower 95% limits of agreement

bility surface area product (nPS) values, respectively, 97 patients with brain tumors. The mean and the difference of results obtained with the two methods (PWI and CTP) are reported on *x*-axis and *y*-axis, respectively. The solid line corresponds to bias. The dashed lines indicate the upper and the lower 95% limits of agreement

population evaluated, pharmacokinetic properties of MRI and CT-specific contrast agents [35] and tracer kinetics models used to calculate permeability and the number of phases chosen for CTP acquisition were different. DCE-PWI K^{trans} is considered the parameter of choice for measuring permeability since it describes accurately the amount of contrast that leaks from vessels into extravascular interstitial space across the BBB by its relationship with extraction fraction (*E*), the quotient of the contrast that extravasates from intravascular space into extravascular space, blood flow and PS [2, 10, 36]. Conversely, K2 indicates the volume of contrast that moves from extravascular interstitial space into vessels through the BBB and may not correlate linearly with the permeability due to a complex relationship between tissue contrast concentration and the changes in signal intensity, potentially leading to inaccurate estimations of microvascular permeability in highly leaky tumors [7, 37, 38]. For CTP, a two-phase protocol is recommended due to its ability to take into account the bidirectional diffusion of contrast agent between the extravascular and intravascular space with a longer acquisition time compared to a one-phase protocol [2, 10]. The present study has some limitations. The sample size of the three patient groups is disproportionate due to the small number of patients with low-grade gliomas and solitary metastases. However, this reflects a real-world setting in which high gliomas are more frequent than low-grade gliomas and isolated brain metastases. Additionally, DSC-PWI K2 maps is not the most robust method for determining microvascular permeability, but it weakly correlates with K^{trans} and is consistent in measuring tumor permeability [6]. Finally, post-processing leakage correction was not associated with preload dose of contrast agent for obtaining a synergistic effect in the improvement of the accuracy and precision of CBV computation, as recently proposed

[3]. Nonetheless, the use of contrast prebolus remains still controversial since it may impact the estimation of permeability [30].

Conclusion

Taken together, our findings suggest that DSC-PWI and CTP CBF and CBV maps are comparable and interchangeable in the evaluation of tumor vascularity, whereas DSC-PWI K2 and CTP PS maps are more discordant in the calculation of tumor permeability in primary and secondary brain malignancies. Thus, despite dose exposition concerns, CTP could be an alternative method for reliably quantifying tumor neoangiogenesis when MRI is not available. Additionally, CTP is suitable when MRI cannot be performed due to patient contraindications or in case the patient does not tolerate it. Therefore, further studies in a larger and more homogeneous patient population of the groups are warranted to clarify the actual role of CTP in brain tumors.

Authors' contributions All authors designed, wrote, and reviewed this article. All authors read and approved the final manuscript.

Funding None.

Availability of data and materials Data available on request at the authors' institution.

Code availability Not applicable.

Declarations

Conflict of interest The authors declare that they have no conflict of interest.

Ethics approval All procedures performed in studies involving human participants were in accordance with the ethical standards of the institutional and/or national research committee and with the 1964 Helsinki Declaration and its later amendments or comparable ethical standards.

Consent to participate All patients have signed consent forms agreeing that their images and data could be used for educational and research purposes.

Consent for publication Obtained.

References

- Griffith B, Jain R (2016) Perfusion imaging in neuro-oncology: basic techniques and clinical applications. *Magn Reson Imaging Clin N Am* 24:765–779
- Eilaghi A, Yeung T, d'Este C et al (2016) Quantitative perfusion and permeability biomarkers in brain cancer from tomographic CT and MR images. *Biomark Cancer* 8(Suppl 2):47–59
- Boxerman JL, Quarles CC, Hu LS et al (2020) Consensus recommendations for a dynamic susceptibility contrast MRI protocol for use in high-grade gliomas. *Neuro Oncol* 22:1262–1275
- Thompson G, Mills SJ, Stivaros SM et al (2010) Imaging of brain tumors: perfusion/permeability. *Neuroimaging Clin N Am* 20:337–353
- Geer CP, Simonds J, Anver A et al (2012) Does MR perfusion imaging impact management decisions for patients with brain tumors? A prospective study. *AJNR Am J Neuroradiol* 33:556–562
- Skinner JT, Moots PL, Ayers GD et al (2016) On the Use of DSC-MRI for measuring vascular permeability. *AJNR Am J Neuroradiol* 37:80–87
- Boxerman JL, Schmainda KM, Weisskoff RM (2006) Relative cerebral blood volume maps corrected for contrast agent extravasation significantly correlate with glioma tumor grade, whereas uncorrected maps do not. *AJNR Am J Neuroradiol* 27:859–867
- Fainardi E, Di Biase F, Borrelli M et al (2010) Potential role of CT perfusion parameters in the identification of solitary intra-axial brain tumor grading. *Acta Neurochir Suppl* 106:283–287
- Jain R (2011) Perfusion CT imaging of brain tumors: an overview. *AJNR Am J Neuroradiol* 32:1570–1577
- Yeung TP, Bauman G, Yartsev S et al (2015) Dynamic perfusion CT in brain tumors. *Eur J Radiol* 84:2386–2392
- Yeung TP, Wang Y, He W et al (2015) Survival prediction in high-grade gliomas using CT perfusion imaging. *J Neurooncol* 123:93–102
- Gadda D, Simonelli P, Villa G et al (2011) Intracranial masses with perilesional edema: differential diagnosis with Perfusion CT. *Neuroradiol J* 24:345–349
- De Simone M, Muccio CF, Pagnotta SM et al (2013) Comparison between CT and MR in perfusion imaging assessment of high-grade gliomas. *Radiol Med* 118:140–151
- Coolens C, Driscoll B, Foltz W et al (2016) Comparison of voxel-wise tumor perfusion changes measured with dynamic contrast-enhanced (DCE) MRI and volumetric DCE CT in patients with metastatic brain cancer treated with radiosurgery. *Tomography* 2:325–333
- Jia ZZ, Shi W, Shi JL et al (2017) Comparison between perfusion computed tomography and dynamic contrast-enhanced magnetic resonance imaging in assessing glioblastoma microvasculature. *Eur J Radiol* 87:120–124
- Østergaard L, Sorensen A, Kwong K et al (1996) High resolution measurement of cerebral blood flow using intravascular tracer bolus passages. Part II: experimental comparison and preliminary results. *Magnet Reson Med* 36:726–736
- Cenic A, Nabavi DG, Craen RA et al (2000) A CT method to measure hemodynamics in brain tumors: validation and application of cerebral blood flow maps. *AJNR Am J Neuroradiol* 21:462–470
- Yeung TPC, Yartsev Y, Lee TY et al (2014) Relationship of computed tomography perfusion and positron emission tomography to tumour progression in malignant glioma. *J Med Radiat Sci* 61:4–13
- Luan J, Wu M, Wang X et al (2020) The diagnostic value of quantitative analysis of ASL, DSC-MRI and DKI in the grading of cerebral gliomas: a meta-analysis. *Radiat Oncol* 15:204
- Hakyemez B, Erdogan C, Ercan I et al (2005) High-grade and low-grade gliomas: differentiation by using perfusion MR imaging. *Clin Radiol* 60:493–502
- Server A, Graff BA, Orheim TE et al (2011) Measurements of diagnostic examination performance and correlation analysis using microvascular leakage, cerebral blood volume, and blood flow derived from 3T dynamic susceptibility-weighted contrast-enhanced perfusion MR imaging in glial tumor grading. *Neuroradiology* 53:435–447
- Waqar M, Lewis D, Agushi E et al (2021) Cerebral and tumoral blood flow in adult gliomas: a systematic review of results from magnetic resonance imaging. *Br J Radiol* 194:20201450
- Provenzale JM, Wang GR, Brenner T et al (2002) Comparison of permeability in high-grade and low-grade brain tumors using dynamic susceptibility contrast MR imaging. *AJR Am J Roentgenol* 178:711–716
- Jain R, Griffith B, Alotaibi F et al (2015) Glioma angiogenesis and perfusion imaging: understanding the relationship between tumor blood volume and leakiness with increasing glioma grade. *AJNR Am J Neuroradiol* 36:2030–2033
- Cindil E, Sendur HN, Cerit MN et al (2021) Validation of combined use of DWI and percentage signal recovery-optimized protocol of DSC-MRI in differentiation of high-grade glioma, metastasis, and lymphoma. *Neuroradiology* 63:331–342
- Lee YJ, Ahn KJ, Kim BS et al (2012) Role of perfusion CT in differentiating between various cerebral masses using normalized permeability surface area product and cerebral blood volume. *Clin Imaging* 36:680–687
- Onishi S, Kajiwara Y, Takayasu T et al (2018) Perfusion computed tomography parameters are useful for differentiating glioblastoma, lymphoma, and metastasis. *World Neurosurg* 119:e890–e897
- Mangla R, Kolar B, Zhu T et al (2011) Percentage signal recovery derived from MR dynamic susceptibility contrast imaging is useful to differentiate common enhancing malignant lesions of the brain. *AJNR Am J Neuroradiol* 32:1004–1010
- Lu S, Gao Q, Yu J et al (2016) Utility of dynamic contrast-enhanced magnetic resonance imaging for differentiating glioblastoma, primary central nervous system lymphoma and brain metastatic tumor. *Eur J Radiol* 85:1722–1727
- Server A, Orheim TE, Graff BA et al (2011) Diagnostic examination performance by using microvascular leakage, cerebral blood volume, and blood flow derived from 3-T dynamic susceptibility-weighted contrast-enhanced perfusion MR imaging in the differentiation of glioblastoma multiforme and brain metastasis. *Neuroradiology* 53:319–330
- Xyda A, Haberland U, Klotz E et al (2012) Diagnostic performance of whole brain volume perfusion CT in intra-axial brain tumors: preoperative classification accuracy and histopathologic correlation. *Eur J Radiol* 81:4105–4111
- Jain RK, di Tomaso E, Duda DG et al (2007) Angiogenesis in brain tumours. *Nat Rev Neurosci* 8:610–622

33. Cacho-Díaz B, García-Botello DR, Wegman-Ostrosky T et al (2020) Tumor microenvironment differences between primary tumor and brain metastases. *J Transl Med* 18:1
34. Paulson ES, Schmainda KM (2008) Comparison of dynamic susceptibility-weighted contrast-enhanced MR methods: recommendations for measuring relative cerebral blood volume in brain tumors. *Radiology* 249:601–613
35. Choyke PL (2005) Contrast agents for imaging tumor angiogenesis: is bigger better? *Radiology* 235:1–2
36. Heye AK, Culling RD, Valdés Hernández MDC, Thrippleton MJ, Wardlaw JM (2014) Assessment of blood-brain barrier disruption using dynamic contrast-enhanced MRI. A systematic review. *Neuroimage Clin* 6:262–274
37. Rimmer A, Holodny AI, Hochberg FH (2006) Perfusion magnetic resonance imaging to assess brain tumor responses to new therapies. *US Neurol Dis* 1:1–6
38. Cha S, Yang L, Johnson G et al (2006) Comparison of microvascular permeability measurements, Ktrans, determined with conventional steady-state T1-Weighted and first-pass T2*-Weighted MR imaging methods in gliomas and meningiomas. *AJNR Am J Neuroradiol* 27:409–417

Publisher's Note Springer Nature remains neutral with regard to jurisdictional claims in published maps and institutional affiliations.